Journal of Constructional Steel Research 89 (2013) 165–174

Contents lists available at ScienceDirect

Journal of Constructional Steel Research

Performance based robust design optimization of steel moment resisting frames

Zhifeng Liu, Sez Atamturktur *, C. Hsein Juang

Glenn Department of Civil Engineering, Clemson University, Clemson, SC 29634, United States

ARTICLE INFO

Article history:
Received 31 January 2013
Accepted 1 July 2013
Available online 1 August 2013

Keywords:
Robust design
Multi-objective optimization
NSGA-II
Pareto front
Demand and capacity factor design
Uniformity drift ratio

ABSTRACT

The seismic design of steel-moment resisting frames is subjected to uncertainties originating from various sources including imprecisely known seismic load, inaccurate modeling assumptions, as well as uncertain material properties and connection behavior. These uncertainties must be considered in the structural design process to ensure that a safe design is achieved. Design codes based on reliability of performance are useful in providing safety margins for the performance objectives with quantifiable confidence levels considering various sources of uncertainties. In these design codes, although seismic demand is usually calculated with a suite of ground motions, only the median seismic demand is used in the subsequent calculation of acceptance criterion (i.e., confidence level), and variation in seismic demand is not used. In the present manuscript, the authors utilize a performance based design approach for seismic design optimization of steel moment resisting frames, where material weight, mean value of seismic demand and variation of seismic demand are treated as three design objectives representing the cost, safety and robustness measures, respectively. Through a case study application, the proposed methodology is demonstrated to be capable of providing a set of Pareto-optimal designs with competing cost, safety and robustness. The obtained Pareto front designs are utilized in the development of *uniformity drift ratio* as design efficiency indicator. Required uniformity drift ratio to ensure efficient designs for each range of maximum inter-story drift is suggested based on the obtained results. Finally, the influence of the selected connection model and the response modification factor on the obtained results is investigated.

1. Introduction

Traditional steel moment resisting frame design, by its nature is a trial and error process seeking designs that are both safe and economical. Safety concerns are mitigated by compliance to the reliability based design standards (e.g., ASCE 7 [1], AISC 360 [2], and FEMA 350 [3]), while economic concerns are typically evaluated considering the initial construction cost. The structural designer then selects a design from several code-compliant candidate designs, according to the cost and other project related factors. Since only a finite number of candidate designs can be evaluated given the unavoidable limitations on the design budgets and the designers' effort, the acquired design is likely not to be the most optimal in its cost and/or safety.

Steel moment resisting frame design optimization, in previous research efforts, is treated as either a single [4–7] or a multi-objective optimization problem [8–12]. In single objective optimization, in most cases, cost is treated as the only objective, while building code and other project requirements are treated as constraints. Optimization algorithm is then used to reach designs that satisfy the project requirements with minimal cost. The tedious trial-and-error process, which is customarily handled by the structural designer, is performed by a computer algorithm with the entirety of the design space being explored in search for the most optimal design. In multi-objective optimization however, other criteria, such as the number of steel sections [10] can also be considered simultaneously with cost. For instance, Sarma and Adeli [8] proposed a life cycle cost optimization problem for steel structures with four optimization criteria: steel section cost, steel section weight, the number of steel section types, and perimeter length (to account for painting cost in life time).

Seismic design of steel moment resisting frames has been studied extensively through optimization based techniques. Liu et al. [9] optimized initial material cost and life-cycle cost simultaneously considering AISC-LRFD seismic provisions and 1997 NEHRP requirement as constraints. Fragiadakis et al. [11] optimized steel material weight and life-cycle costs using Eurocode 3 and Eurocode 8 requirements as constraints. Rojas et al. [12] minimized both weight and expected annual building replacement cost of steel moment-resisting frames simultaneously, with performance objective confidence level requirement as constraint.

One aspect that has received little attention in the published literature is the fact that due to the inherent uncertainty in the construction

Abbreviations: RDO, robust design optimization; IO, immediate occupancy; CP, collapse prevention; NSGA-II, non-dominated sorting genetic algorithm, version II; UDR, uniformity drift ratio.

* Corresponding author. Tel.: +1 8646563003; fax: +1 8646562670.
E-mail address: sez@clemson.edu (S. Atamturktur).

0143-974X/$ – see front matter © 2013 Elsevier Ltd. All rights reserved.
http://dx.doi.org/10.1016/j.jcsr.2013.07.011

and operational conditions of a structure, seismic demand may deviate from expected values. Without considering immunity of seismic demand to uncertainty, one may reach a design that has large sensitivity to uncertainty and thus, large variation in performance. Herein, the immunity to uncertainty is referred to as 'robustness' as originally proposed by Taguchi [13].

The present manuscript proposes a new steel moment resisting frame design optimization approach utilizing robust design, a concept originally developed and widely used in quality engineering [13, 14]. Our approach goes beyond studies that focus on the cost and mean seismic demand, and considers robustness of the seismic demand to uncertainty present in the seismic design process. Maximum inter-story drift is used to assess the seismic demand, and the variability of ground motion is the considered as the source of uncertainty. Hence, the mean value of maximum inter-story drift is used as the *safety* measure; the standard deviation of the maximum inter-story drift is used as the *robustness* measure, and material weight is used to represent the *cost* of the design. A smaller mean value of inter-story drift indicates less demand on the structure, and therefore yields a safer design; while a smaller value of the standard deviation of maximum inter-story drift indicates a more robust design. Therefore, the proposed approach leads to a multi-objective optimization problem resulting in a set of competing designs that are economical, safe and robust.

The present manuscript is organized as follows. The fundamental concept behind robust design is introduced in Section 2, performance-based robust design optimization is discussed in Section 3. Multi-objective optimization methodology implemented herein to solve the robust design optimization problem is overviewed in Section 4. In Section 5, the application of the proposed design approach is demonstrated on a four-story three-bay steel moment resisting frame. In Section 6, a parametric analysis is performed to investigate the effect of the selected connection model and response modification factor on Pareto front solutions. Finally, in Section 7, the conclusions are drawn, limitations are discussed and suggestions for future work are given.

2. Robust design

The purpose of robust design is to make a product or response of a system insensitive to (or robust against) "hard-to-control" input parameters (called "noise factors"), by carefully adjusting "easy-to-control" input parameters (called "design parameters" or "control factors"). Robust design has successfully been used in industrial and manufacturing engineering to produce high quality products and processes. Two kinds of approaches are most widely used in robust design: (i) the Taguchi method and its variants [13, 14], and (ii) the robust design optimization method [15].

The Taguchi method, fundamentally an experimental design approach, is characterized by an orthogonal array with design parameters and noise factors assigned to inner and outer arrays, respectively [14]. For each set of design parameters, several experiments with different combinations of noise factors determined from the outer array are performed. Subsequently the analysis of mean is performed to characterize design parameters into four categories: (i) design parameters affecting mean and variance of the response, (ii) design parameters affecting variance only, (iii) design parameters affecting mean only, and (iv) design parameters affecting cost only. Design parameters of the first two categories are adjusted to reduce variance; the third category is adjusted to move the mean value of the response to the target value and the last category is adjusted to reduce cost [14]. Though easy to implement, the following limitations of the Taguchi method have made it the subject of criticism [16]: (1) design parameters cannot always be grouped into four distinct categories; and (2) due to the inherent experimental nature of the design, only a select few designs may be evaluated and compared, prohibiting a thorough exploration of the design space.

With the development of computational capabilities and progress in the optimization techniques, robust design optimization (RDO) has gained popularity (Beyer and Sendhoff 2007) [17]. The three goals formulate the robust design, i.e., reducing variance in system response, reducing cost and bringing mean value of system response to the target, leads naturally to a multi-objective optimization problem. In some cases, the target value for the mean is specific; in others, the mean value is either maximized or minimized. RDO is advantageous as it can explore the entire solution space to find the most optimum design and straightforwardly evaluate highly nonlinear problems. In the present study, RDO is adopted for the performance based seismic design of steel moment resisting frames.

3. Performance based robust design

Many sources of uncertainties exist in performance based seismic design [18]. For instance, seismic hazard varies due to the attenuation laws employed. For given seismic intensity, seismic demand parameters vary from record-to-record, known as ground motion variability. Moreover, uncertainty also exists in structural modeling owing to the unavoidable simplifications made and assumptions established in the numerical analysis, such as using center-line model instead of precisely modeling the panel zone; employing a 2D model instead of considering the 3D effects; and using inaccurately estimated damping ratio or employing inaccurate connection models.

Unlike traditional seismic design method, in which preventing fatality through ensuring an acceptably low collapse probability is the main goal, in performance based design, performance is divided into several levels each corresponding to a seismic hazard level. FEMA 350 supplies a probability based guideline for performance based design of steel moment resisting frames, in which the ground motion variability and the uncertainty in the structural analysis are considered explicitly. FEMA 350 considers two performance levels, immediate occupancy (IO) and collapse prevention (CP), corresponding to 50% probability of being exceeded in 50 years and 2% probability of being exceeded in 50 years, respectively. In FEMA 350, performance objective is satisfied probabilistically in that IO performance level has an annual frequency of being exceeded less than 1/100, while CP performance level has an annual frequency of being exceeded less than 1/2500 [3].

Analogous to LRFD design, in FEMA 350, the performance objectives are satisfied by demand and capacity factor design (DCFD) method [19], instead of direct calculation of the annual frequency of being exceeded. DCFD involves calculation of the factored demand to the factored capacity ratio (also known as a confidence parameter), as expressed in Eq. (1):

$$\lambda = \frac{\gamma \cdot \gamma_a \cdot D}{\phi \cdot C}. \tag{1}$$

With λ known, a metric named confidence level can be computed, which quantifies the confidence of performance objective being satisfied in face of the uncertainties due to seismic hazard curve and other epistemic uncertainties [19]. In FEMA 350, minimum confidence level for IO and CP performance objective is suggested as 50% and 90%, respectively.

In Eq. (1), only median seismic demand, D is used. This is due to the following assumption established in FEMA 350: record to record variability, i.e. standard deviation of logarithm value of seismic demand under given seismic intensity, is a constant value of 0.3 [19]. This assumption, which eliminates the need to compute record to record variability case by case has not been validated raising the following question: for identical median seismic demand, what is the extent to which the seismic demand variation is affected by the design parameters? If the effect of design parameters on the variation of seismic demand is significant, then for a given median seismic demand,

one can seek for design parameters that reduce the variation of seismic demand, yielding a more *robust* design. This potential reduction in seismic demand variation is not evaluated previously in the established literature and is the objective of the present manuscript.

In this manuscript, the authors apply the principles of robust design optimization to performance based design of steel moment resisting frames. The design variables are the steel section sizes, while seismic demand, i.e. system response of interest, is the maximum inter-story drift. Inter-story drift is closely related to both local and global stability, as well as P-Δ effects [20]. The mean value of maximum inter-story drift, μ_{drift} is considered as the *safety* measure and the standard deviation of maximum inter-story drift, σ_{drift} is considered as the *robustness* measure. For the *cost* measure, initial construction cost, represented by steel material weight is adopted [10]. Ground motion variability, a significant contributor to seismic demand variation for steel moment resisting frame [21], is treated as the noise factor. The AISC 360 requirements, ASCE 7 requirement, and FEMA 350 acceptance criteria are implemented as design constraints. The performance based robust design optimization of steel moment resisting frame problem is expressed as follows:

$$\begin{aligned}&\text{Find } d \text{ to minimize}: \left\{W(d), \mu_{drift}(d,z), \sigma_{drift}(d,z)\right\}\\ &\text{Subject to}:\\ &\text{AISC 360 Code Requirements};\\ &\text{ASCE 7 Code Requirements};\\ &\text{FEMA350 Acceptance Criteria}: \text{CP performance confidence level} > 0.9;\\ &\qquad\qquad\qquad\qquad\text{IO performance confidence level} > 0.5\end{aligned}$$

where W is the steel material weight, d is the design parameters (steel section types), z is the noise factor (ground motion variability). It should be noted that, only μ_{drift} and σ_{drift} under 2% probability of being exceeded in 50 years seismic hazard level are treated as design objectives, since the consequence of exceeding CP performance is more detrimental.

AISC 360 is employed in member detailing. The following requirements are imposed: (1) member strength requirement to limit member stress; (2) strong column weak beam criteria requirement to avoid weak story mechanism; (3) width-thickness ratio limit requirement to prevent buckling of the members; and (4) stability requirement. Furthermore, the following load combinations are considered according to ASCE7-10:

$$\begin{aligned}&1.4DL\\ &1.2DL + 1.6LL + 0.5LL_r\\ &(1.2 + 0.2S_{DS})DL + \rho Q_E + 0.5LL\\ &(0.9-0.2S_{DS})DL + \rho Q_E\end{aligned} \tag{2}$$

in which DL, LL, LL_r, and Q_E, are the dead load, live load, roof live load, and earthquake load, respectively; S_{DS} is the elastic response spectral acceleration at short period; and ρ is the redundancy factor.

4. Methodology: multi-objective optimization and non-dominated sorting genetic algorithm II

In general, a multi-objective optimization problem can be expressed as:

$$\begin{aligned}&\text{Minimize}: \quad F(d) = [f_1(d), f_2(d), \ldots, f_l(d)]\\ &\text{Subject to}: \quad g_i(d) \le 0 \quad i = 1, \ldots, n\end{aligned} \tag{3}$$

with f representing a single objective function, and g representing a constraint function. Unlike single objective optimization, the purpose of which is to search for a single best design, multi-objective optimization yields a family of optimum designs. When the objectives are uncooperative (or conflicting), a single design optimum for all objectives does not exist in the solution space, which is represented by an unattainable, imaginary point known as the *utopia point* in Fig. 1. There generally exists a set of designs in the solution space (i.e., set {F(d) | g_i(d) ≤ 0 for all i}), which are superior to all other designs, while within this set, no design is superior to another in all criteria. These designs constitute a Pareto optimum set (or Pareto front), as illustrated in Fig. 1.

Hence, the Pareto front can be viewed as a set of designs, which dominate all other designs. The *domination relationship* is defined as follows: design B is dominated by design A, if A is superior to B in at least one criteria (i.e., $f_i(d)_A < f_i(d)_B$ for at least one i), and A is not inferior to B in all other criteria (i.e., $f_i(d)_A \le f_i(d)_B$ for all other i). If one design is not dominated by any other designs, it belongs to the Pareto front. A Pareto front has the following features: (1) Within the Pareto front, no improvement is possible in one objective without worsening other objectives. Thus, the Pareto front represents a trade-off relationship, in which objectives compete with each other. (2) All other designs in the solution space are known as dominated designs, which are dominated by at least one design in the Pareto front.

Various optimization methods, such as weighted sum method [22], goal programming [23], compromise programming [24], physical programming [25], and non-dominated sorting genetic algorithm II (NSGA-II) [26] have been proposed for solving multi-objective optimization problems, a comprehensive survey of which is provided by Marler and Arora [27]. Among the available methods, the NSGA-II presents distinct advantages. Being a population-based optimization method, NSGA-II operates on a group of designs rather than one design; thus, Pareto front can be acquired with a single run. Furthermore, NSGA-II is demonstrated to be capable of identifying Pareto front designs in a computationally efficient manner [26]. For those reasons, NSGA-II is adopted here.

5. Steel moment resisting frame case study

5.1. Prototype structure

The proposed performance based robust design optimization is illustrated on a four-story three-bay steel moment resisting frame assumed to be located in Los Angeles, California (Fig. 2). The two-dimensional frame system in east–west direction is employed as illustrative example, with an assumed dead load of 70 psf (3.35 kPa) for the floor and 56 psf (2.68 kPa) for the roof including the weight of slabs. The live load is assumed to be 40 psf (1.91 kPa) for floor levels and 15 psf (0.72 kPa) for roof level, and the external wall load is assumed to be 30 psf (1.44 kPa) for all levels. A572 grade 50 ksi steel is used for all beams and columns. All beams at the

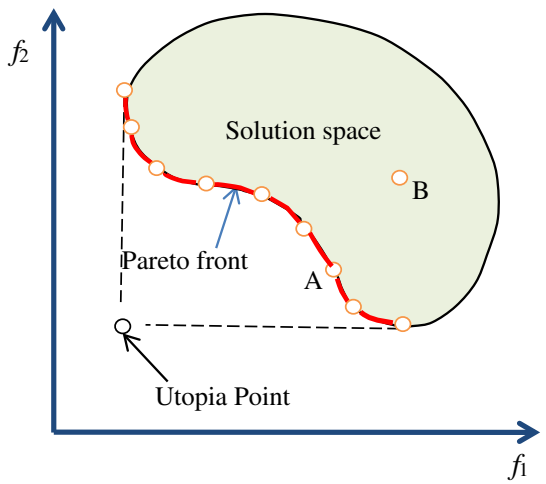

Fig. 1. Pareto front in a bi-objective space (Gencturk and Elnashai, 2011).

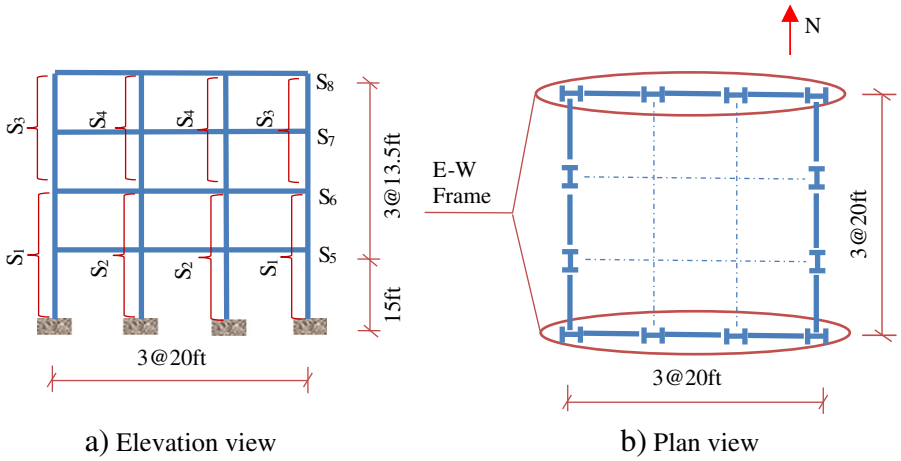

Fig. 2. Elevation view and plan view of the example steel moment resisting frame.

same floor level are grouped into the same section type, and the columns of two adjacent floors symmetric with respect to the vertical center line are grouped together (Fig. 2). This grouping results in a total of eight section types, i.e., eight design parameters. During optimization, steel sections are selected from the list of commonly used sections in tradition steel moment resisting frame design given in Table 1.

5.2. Ground motion uncertainty

The set of ground motions for 50%/50year and 2%/50year seismic hazard level developed for the Los Angeles SAC project is employed [28]. The ground motions has been scaled to match the 50%/50 year and 2%/50 year uniform hazard spectrums through least-square minimization at 0.5 s, 1 s, 2 s and 4 s. The characteristics of these twenty motions for 2%/50 seismic hazard level are shown in Table 2 with a type D soil assumed. Based on the assumption that seismic data can be well described with lognormal distribution, the median, 84th percentile, 16th percentile elastic spectrum acceleration (S_a) and spectrum displacement (S_d) with 5% damping are calculated as shown in Fig. 3.

5.3. Structural model

In the established literature, four distinct analysis procedures are available to compute seismic demand: the linear static method, the linear dynamic method, the nonlinear static method and the nonlinear dynamic method. Though the nonlinear dynamic method is the most rigorous and accurate, it also is the most computationally intensive. Nonlinear static analysis, also known as nonlinear push over analysis, is an efficient alternative to nonlinear dynamic analysis, in which a lateral distributed force is applied to the structure with increasing magnitude until the target roof displacement is reached. The displacement coefficient method in FEMA 356 and capacity spectrum method in ATC-40 [29, 30] are the most commonly used nonlinear static analysis procedures [31]. Improved procedures for displacement coefficient method and capacity spectrum method are also provided in FEMA 440 [32]. In these methods however, the effect of higher order modes and the force redistribution from structural yielding are not considered. As such, the accuracy of the pushover analysis has been a subject of criticism.

The modal pushover analysis (MPA) procedure proposed by Chopra and Goel [33] supplies an improved accuracy compared to the pushover analysis and is proven to be capable of predicting seismic demands similar to the rigorous nonlinear dynamic analysis with much less computational effort [33]. The effort for MPA can be reduced significantly by assuming higher order modes to be elastic without sacrificing accuracy in a significant way [34], referred to as modified MPA. Due to its computational efficiency and favorable accuracy, modified MPA is adopted here to calculate seismic demand.

Pushover analysis of the full frame and nonlinear dynamic analysis of the idealized inelastic single degree of freedom system of the first mode are performed with open system for earthquake engineering simulation (OpenSEES). 'nonlinearBeamColumn' element with a strain

Table 1
List of columns and beams.

Column		Beam	
W14 × 99	W14 × 211	W24 × 55	W33 × 116
W14 × 109	W14 × 233	W24 × 62	W33 × 130
W14 × 120	W14 × 257	W24 × 68	W33 × 141
W14 × 132	W14 × 283	W24 × 76	W33 × 152
W14 × 145	W14 × 311	W27 × 84	W36 × 135
W14 × 159	W14 × 342	W27 × 94	W36 × 150
W14 × 176	W14 × 370	W27 × 102	W36 × 160
W14 × 193	W14 × 398	W27 × 114	W36 × 170

Table 2
Characteristics of the ground motions at 2%/50 year seismic hazard level.

Name	Record	Magnitude	Distance (km)	Scale factor	PGA (g)
LA21	1995 Kobe	6.9	3.4	1.15	1.258
LA22	1995 Kobe	6.9	3.4	1.15	0.903
LA23	1989 Loma Prieta	7	3.5	0.82	0.41
LA24	1989 Loma Prieta	7	3.5	0.82	0.464
LA25	1994 Northridge	6.7	7.5	1.29	0.852
LA26	1994 Northridge	6.7	7.5	1.29	0.925
LA27	1994 Northridge	6.7	6.4	1.61	0.909
LA28	1994 Northridge	6.7	6.4	1.61	1.304
LA29	1974 Tabas	7.4	1.2	1.08	0.793
LA30	1974 Tabas	7.4	1.2	1.08	0.973
LA31	Elysian Park (simulated)	7.1	17.5	1.43	1.271
LA32	Elysian Park (simulated)	7.1	17.5	1.43	1.164
LA33	Elysian Park (simulated)	7.1	10.7	0.97	0.767
LA34	Elysian Park (simulated)	7.1	10.7	0.97	0.668
LA35	Elysian Park (simulated)	7.1	11.2	1.1	0.973
LA36	Elysian Park (simulated)	7.1	11.2	1.1	1.079
LA37	Palos Verdes (simulated)	7.1	1.5	0.9	0.698
LA38	Palos Verdes (simulated)	7.1	1.5	0.9	0.762
LA39	Palos Verdes (simulated)	7.1	1.5	0.88	0.491
LA40	Palos Verdes (simulated)	7.1	1.5	0.88	0.613

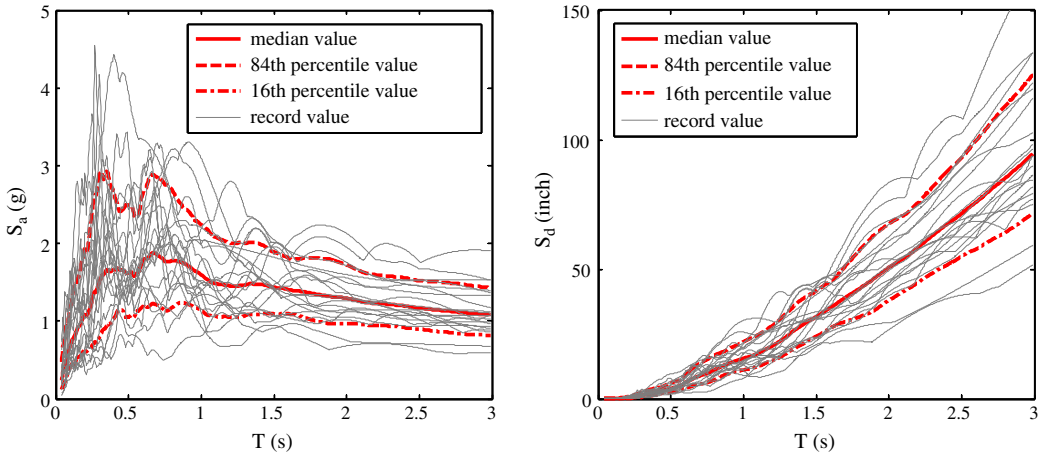

Fig. 3. S_a and S_d response spectrum for 2% 50 year seismic hazard level Los Angeles ground motions with 5% damping.

hardening ratio of 3% is used to simulate the columns. The nonlinearity of the beam elements is modeled with Ibarra–Krawinkler (IK) model [35], characterized by three strength parameters [M_y: effective yield moment; M_c: capping moment (post yield strength ratio defined as M_c/M_y); and residual moment: $M_r = \kappa M_y$], four deformation parameters [θ_y: yield rotation; θ_p: pre-capping plastic rotation; θ_{pc}: post-capping plastic rotation; and θ_u: ultimate plastic rotation capacity], and one cyclic deterioration parameter (Fig. 4). The parameters for steel sections can be predicted with regression equations provided by Lignos and Krawinkler [36] that are expressed as functions of geometric parameters and yield strength of the steel section. θ_u however, is highly dependent on load history and difficult to determine accurately. For beams under stepwise increasing cyclic load, θ_u is reported to be between 0.05 and 0.06 rad [36] and in this study, θ_u is assumed to be 0.06 rad. Moreover, P-Δ effect is modeled with fictitious column approach [37].

5.4. Interpretation of the results

The formulated optimization problem is solved through NSGA-II by evaluating 500 designs in each generation with a total number of 50 generations. The converged solution, i.e., the acquired Pareto front of the last generation, is shown in Fig. 5. For comparison purposes, Fig. 5 also depicts the feasible designs of generation 1. Since no designs belong to Pareto front in generation 1, they are termed as 'dominated designs' in the figure.

5.4.1. Relation between μ_{drift}–cost and σ_{drift}–cost

The design population of the initial generation and the last generation is illustrated in Fig. 5(a). As the σ_{drift}–weight (cost) plot (Fig. 5(b)) clearly indicates, the Pareto front designs are more robust (smaller σ_{drift}) than dominated designs for identical cost. For identical robustness (σ_{drift}), Pareto front designs are more economical than dominated designs. From the μ_{drift}–weight (cost) plot (Fig. 5(c)), the Pareto front designs are observed to exhibit smaller seismic demand (μ_{drift}) compared to the dominated designs for identical cost, while for designs with identical seismic demand (μ_{drift}), the Pareto front designs are more economical than the dominated designs.

In general, for given cost, both μ_{drift} and σ_{drift} can be greatly optimized, i.e., with steel weight as 80,000 lb (36,320 kg), σ_{drift} can be improved from the worst case of 1.6% in dominated designs to the best case of less than 0.6% in Pareto front, and μ_{drift} can be improved from the worst case of 3.7% in dominated design to the best case of around 1.5% in Pareto front. For identical μ_{drift} or σ_{drift}, cost of the designs can also be greatly optimized, i.e., with μ_{drift} as 2%, steel weight can be reduced from the worst case of 100,000 lb (45,400 kg) in dominated designs to the best case of 71,000 lb (32,234 kg) in Pareto

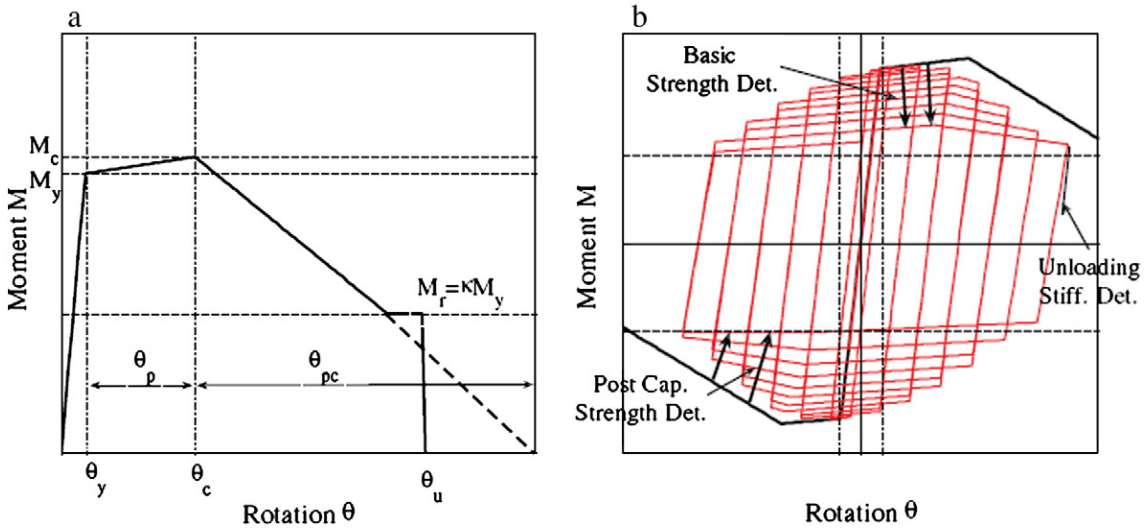

Fig. 4. Modified IK deterioration model.

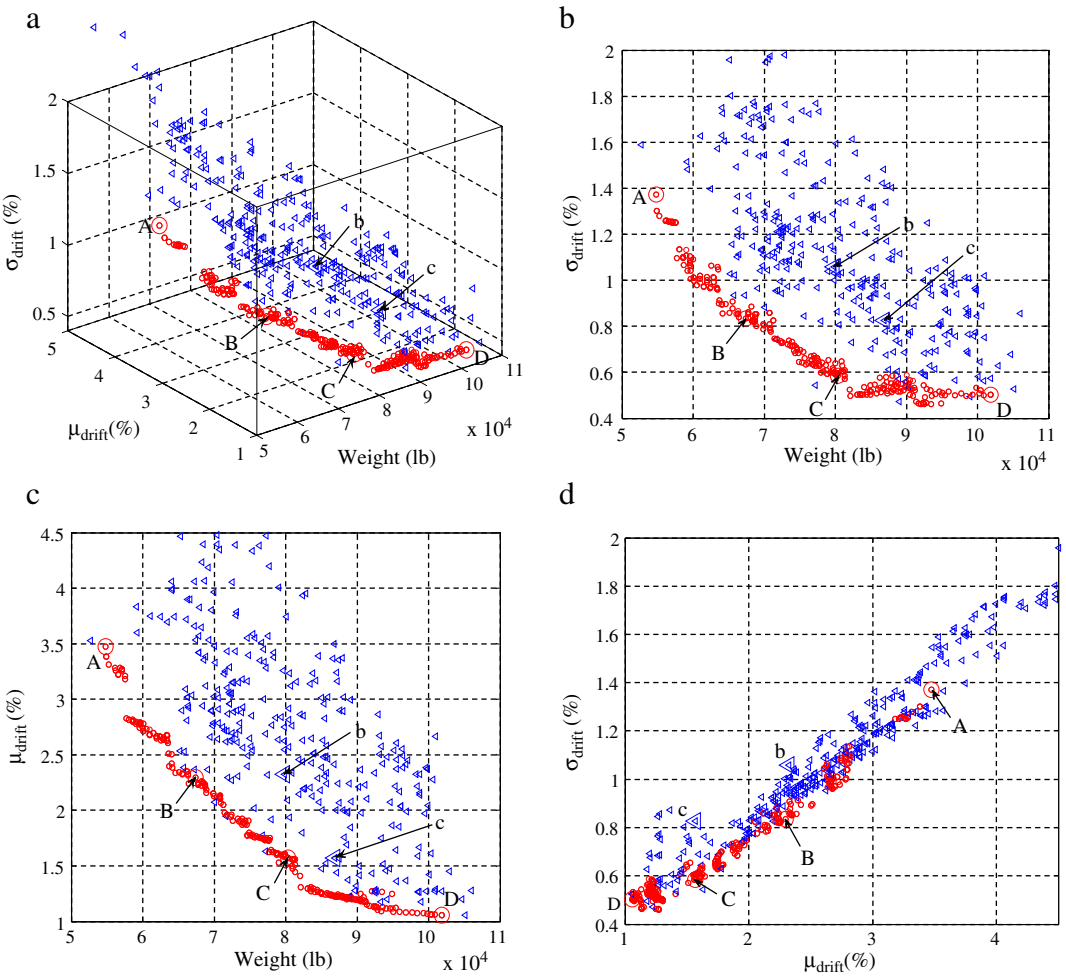

Fig. 5. Pareto front and dominated designs.

front; with σ_{drift} as 1%, steel weight can be reduced from the worst case as 100,000 lb (45,400 kg) in dominated designs to the best case as 60,000 lb (27,240 kg) in Pareto front.

In the first generation, designs are randomly generated and the code-compliant designs are selected as feasible designs—similar to the trial and error process of inexperienced designers. The implication is that though trial and error process can yield code-compliant designs, these designs are far from being optimum. The designs of the first generation can be improved in terms of both robustness (σ_{drift}) and cost as observed from Fig. 5(b) and in terms of both seismic demand (μ_{drift}) and cost as observed from Fig. 5(c).

Six designs are selected for comparison, for which the steel sections and objective function values are listed in Table 3. Designs A, B, C and D are selected from the Pareto front, while Designs b and c are dominated designs. Designs A and D are the lightest design and the heaviest design in Pareto front, respectively. Designs A, B, C and D reflect the tradeoff relationship between cost and safety: comparing the four designs, the design with smaller μ_{drift} will inevitably cost more, and the design with less cost inevitably has larger μ_{drift}. With the tradeoff relationship between cost and μ_{drift}, more informed decision making can be achieved. In single objective optimization, potential changes in safety or robustness due to an increase or decrease of project cost are not supplied. With Pareto front, however, this information becomes readily available. For instance, comparing designs A and C, with material weight increase from 54,792 lb (24,876 kg) to 80,361 lb (36, 484kg) (by 46.7%), the μ_{drift} will be reduced from 3.48%

Table 3
Steel section size and objective values of selected designs (1 lb = 0.454 kg).

Selected designs		Design A	Design B	Design b	Design C	Design c	Design D
Columns	S_1	W14 × 159	W14 × 159	W14 × 211	W14 × 211	W14 × 283	W14 × 398
	S_2	W14 × 193	W14 × 342	W14 × 398	W14 × 398	W14 × 370	W14 × 398
	S_3	W14 × 159	W14 × 159	W14 × 145	W14 × 159	W14 × 99	W14 × 193
	S_4	W14 × 193	W14 × 211	W14 × 193	W14 × 283	W14 × 370	W14 × 398
Beams	S_5	W24 × 76	W27 × 102	W24 × 68	W33 × 116	W36 × 135	W33 × 130
	S_6	W24 × 76	W27 × 102	W36 × 135	W33 × 116	W36 × 160	W33 × 130
	S_7	W24 × 55	W24 × 55	W27 × 84	W24 × 76	W24 × 55	W27 × 94
	S_8	W24 × 55	W24 × 55	W36 × 160	W24 × 55	W24 × 55	W24 × 55
Weight (lb)		54792	67377	79785	80361	86847	101826
μ_{drift}		3.48	2.30	2.32	1.57	1.57	1.06
σ_{drift}		1.37	0.83	1.06	0.58	0.83	0.50

to 1.57% (by 54.9%). As a result, the decision maker has greater control on risk and budget associated with the preferred design. A risk-adverse decision maker may choose a design with smaller μ_{drift} at more expense, while a risk-prone decision maker may choose a design with a greater μ_{drift}. A decision maker may also evaluate the necessary budget for a project when using a Pareto front Liu [9].

5.4.2. Relation between μ_{drift} and σ_{drift}

The data from μ_{drift}–σ_{drift} plot (Fig. 5(d)) indicates that the difference in robustness (σ_{drift}) between the Pareto front designs and the dominated designs is not negligible. Also, the positive correlation of μ_{drift} and σ_{drift} indicates that designs with a larger μ_{drift} also have a larger σ_{drift}.

Comparing Pareto front designs and dominated designs, for identical μ_{drift}, designs in the Pareto front are more robust (smaller σ_{drift}) than dominated designs. For instance, designs C and c have comparative μ_{drift}, while design C is more robust (σ_{drift} of design C is 2/3 of design c), and also more economical (weight of design C is 93% of design c). The implication of these results is that a more robust design is not necessarily more expensive. The same relation is also observed between designs B and b. Thus, for identical μ_{drift}, σ_{drift} can be reduced through adjusting design variables, and a more robust design can be acquired.

In Fig. 6, the cumulative distribution of inter-story drift of the six designs is plotted. From this figure, for each given inter-story drift ratio target, the probability of not being exceeded can be read directly. Comparing designs A, B, C and D, the probability of not being exceeded increases from designs A to D for identical inter-story drift. Comparing designs B and b which have comparable μ_{drift}, for smaller inter-story drift (smaller than 2.7%), design b has larger probability of not being exceeded for identical inter-story drift. For 50% probability of not being exceeded, design B and design b has quite close inter-story drift, since they have close μ_{drift}. However, the probability of not being exceeded of design B exceeds that of design b as the inter-story drift is larger than 2.7%. The same relation between design C and design c is also observed. Thus, for identical μ_{drift}, increasing robustness (reducing σ_{drift}) has the benefit of increasing safety (smaller probability of being exceeded in larger inter-story drift range).

5.4.3. Uniformity drift ratio as a design efficiency indicator

Inter-story drift ratio for all six selected designs of twenty ground motions is plotted in Fig. 7. For each design, the maximum inter-story drift occurs at one or two stories for almost all ground motions,

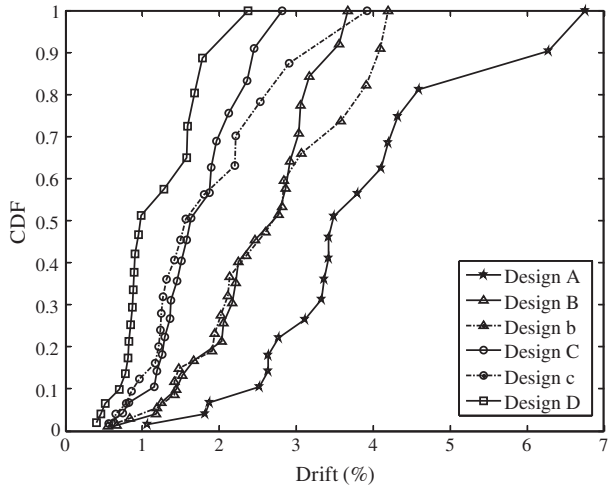

Fig. 6. CDF of inter-story drift of six selected designs.

known as weak stories. It is apparent from both Fig. 7(b) and (c) that maximum inter-story drift of designs b and c exhibits a much greater variance than designs B and C. Furthermore, variation of inter-story drift between different stories of designs B and C is also smaller than that of designs b and c. That is to say designs B and C exhibit a more uniform distribution of the inter-story drift. Though designs b and c are heavier than designs B and C, they are inferior designs, as the inappropriate proportioning of stiffness and strength makes them prone to weak story mechanism failure, i.e., failure due to excessive inter-story drift at one or several stories.

Comparing designs A, B, C and D, the uniformity of the inter-story drift decreases from designs D to A. With larger strength, design D would be within its linear range, whereas design A, as the 'weakest' design yields even when subjected to low intensity ground motion. After yielding, the stiffness is greatly reduced, thusly sharply increasing the displacement with a slight increase in force or ground motion intensity. The large σ_{drift} of designs b and c is also caused by the weak story. As observed from Fig. 7(b), the difference of inter-story drift between different stories is small for low intensity ground motion, while the difference is greatly amplified as ground motion intensity increases after yielding of the first story, resulting in a much larger variation in maximum inter-story drift.

Merely considering maximum inter-story drift is not sufficient to evaluate a design, as story-wise distribution of inter-story drift is not reflected by maximum inter-story drift. The measure uniformity drift ratio (UDR), defined as the ratio of maximum inter-story drift ratio to roof displacement ratio (ratio of roof displacement to building height), can be employed as an indicator of inter-story drift uniformity [10]. According to the definition, UDR should be a value larger than unity, while a smaller UDR indicates a more uniform distribution of inter-story drift.

As for identical cost, Pareto front designs will exhibit smaller μ_{drift}, and for identical μ_{drift}, Pareto front designs will cost less, Pareto front designs are more efficient than dominated designs. As a result, Pareto front designs or almost Pareto front designs (those although are dominated designs but are quite close to the Pareto front) should be pursued. The traditional trial and error based design would most probably result in dominated designs instead of Pareto front designs, as Pareto front designs occupy a small portion of the solution space. Though Pareto front can be acquired by the multi-objective optimization method, the complex programming of optimization is not practical for practicing engineers, thus simplified method for acquiring Pareto front designs or criteria for ensuring efficiency should be explored.

As shown in Fig. 7(c), for design c, the fourth story is weak while the first story is rather strong, resulting in excessive inter-story drift in the fourth story under the case that the first story is essentially within its linear range. Thus, maximum inter-story drift, which is always governed by the weakest story cannot reflect whether strength or stiffness is appropriately proportioned within the building. UDR, however can capture the distribution of strength and stiffness. Generally speaking, for given material weight, a design with more uniform distribution of inter-story drift would most probably have smaller maximum inter-story drift. While for several designs with identical maximum inter-story drift, the one with inter-story drift distributed more uniformly would be expected to distribute strength and stiffness more appropriately, thus would need less material. As a result, UDR is deemed to be a suitable indicator of design efficiency.

To test the applicability of UDR as an efficiency indicator, mean value of UDR of the twenty ground motions for Pareto front designs and dominated designs is calculated, as shown in Fig. 8. UDR is divided into several ranges. The general phenomenon observed is that designs with smaller UDR dominate designs with larger UDR. For every other range of UDR, regions of design are separated clearly, i.e., regions of $1.3 < UDR < 1.4$ and regions of $1.6 < UDR < 1.8$ are not overlapping; the same phenomenon is observed between regions of

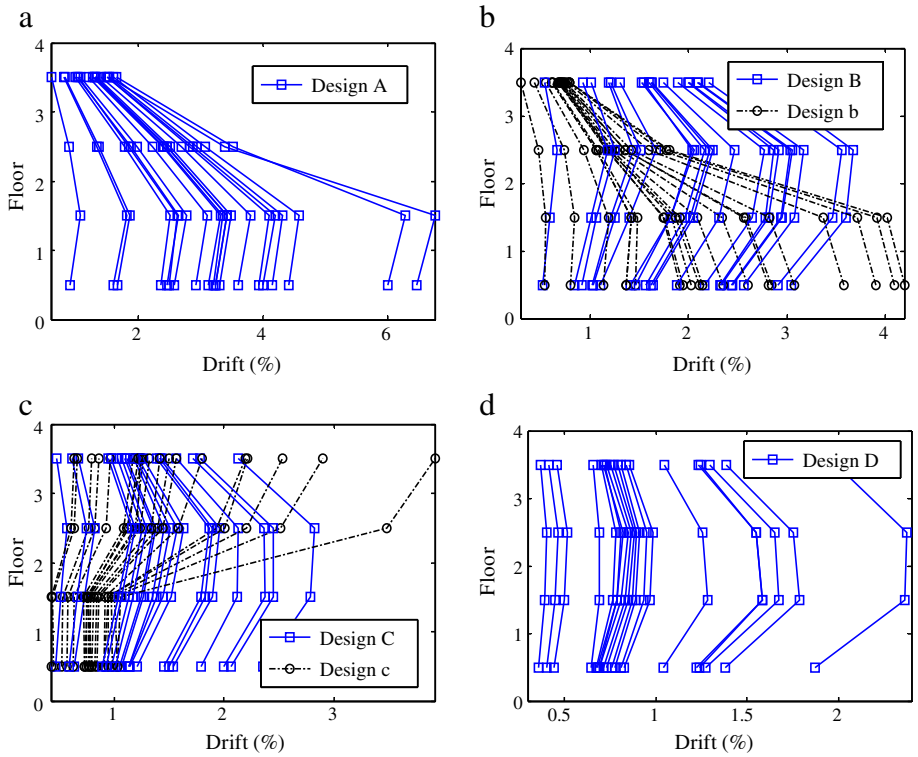

Fig. 7. Inter-story drift ratio results for each ground motion of six selected designs.

1.1 < UDR < 1.2 and regions of 1.3 < UDR < 1.4. Since efficient designs and inefficient designs can be roughly separated with different UDR values, UDR can effectively serve as a design efficiency indicator.

In addition, within Pareto front, designs with larger μ_{drift} generally have larger UDR as well. For μ_{drift} less than 1.2%, all Pareto front designs have a UDR less than 1.1, for μ_{drift} between 1.2% and 2.5%, Pareto front designs have a UDR between 1.1 and 1.2, and for μ_{drift} larger than 2.5%, Pareto front designs have a UDR between 1.2 and 1.3. For larger μ_{drift}, designs would be driven to the nonlinear range more severely, thus resulting in larger difference in maximum inter-story drift between stories, leading to larger UDR.

In trial and error design process, with an acquired design, designers are unaware whether the design is efficient, or whether it can be improved in terms of cost or maximum inter-story drift. As demonstrated here, UDR can serve as the efficiency indicator. A design with UDR as large as 1.8 would be a costly design, and a design with smaller UDR would be a more efficient design. UDR can also serve as criterion to determine whether a design is Pareto front design. Based on distribution of UDR for each range of μ_{drift} in Fig. 8, the following UDR requirement for efficient designs is suggested:

$$\begin{cases} \text{UDR}<1.1 \text{ for } \mu_{drift} < 1.2\%; \\ \text{UDR}<1.2 \text{ for } 1.2\% < \mu_{drift} < 2.5\%; \\ \text{UDR}<1.3 \text{ for } \mu_{drift} > 2.5\%. \end{cases} \tag{4}$$

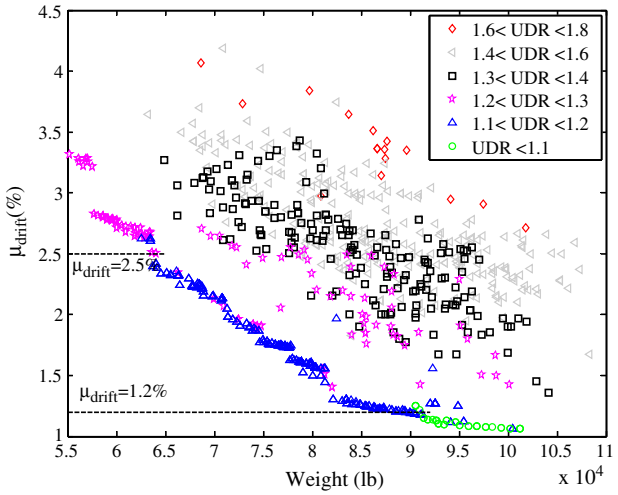

Fig. 8. Uniformity drift ratio distribution for Pareto front designs and dominated designs.

With such range in mind, design efficiency can be determined. With the trial and error design process, trials can be made until a design not only meets code requirement but also satisfies the UDR requirement given in Eq. (4) is found. Thus, with the use of UDR as a guiding efficiency indicator, efficient designs can be achieved without complex optimization. It should be noted that the UDR ranges presented herein are applicable only for the steel frame considered herein. Whether it can be extrapolated to steel moment resisting frame of different stories, or even different structure types need to be verified in future studies. Considering the benefits of appropriately proportioning strength and stiffness, UDR requirement should be considered as a valuable design criterion.

6. Parametric analysis

6.1. Influence of connection behavior

In this section, the results of the effect of the selected connection model on the performance based robust optimization are evaluated. The IK model employed in this research to simulate connection behavior considers both the cyclic deterioration and post-capping behavior and thus, it was reported to accurately predict seismic demand and capacity [35, 36]. There are other connection models available to simulate

nonlinear behavior of beams, however, such as the bilinear model [11, 38], the Fouch and Shi model [39, 40], and Kishi and Chen model [41, 42]. Of these, the bilinear model is the most simplified in its treatment of the mechanics at the connection as it considers neither the cyclic deterioration nor post-capping behavior. Therefore, comparison of robust design optimization results obtained using the most simplified and the most advanced connection models (i.e. the bilinear model and IK model) would reveal the sensitivity of the proposed methodology to the connection model.

In our implementation of the bilinear model, a strain hardening ratio of 3% is assumed, and in our genetic algorithm a population size of 100 is used [10]. In this facet of our work, we overlay both Pareto fronts obtained with the IK and bilinear models, as shown in Fig. 9. Here, the Pareto fronts obtained from these two connection models agree very well in that section sizes of 36 designs coincide identically, suggesting that the dependency of the performance based robust optimization approach on the selected connection model is negligible.

Subsequently, it is observed that μ_{drift} calculated using the bilinear model was in close agreement with μ_{drift} based upon the IK model. The cyclic deterioration and post-capping behavior, which are not considered within the bilinear model, are known to play an important role in evaluating collapse capacity [35, 36]. However, for inter-story drift values much smaller than collapse capacity (i.e., μ_{drift} is smaller than 3% in Fig. 10), the cyclic deterioration and post-capping behavior only marginally influence the predicted structural behavior.

6.2. Influence of response modification factor

The response modification factor, R is the ratio of the force that will be developed in a seismic resistant system if the system remains elastic under design ground motion to the yielding force of the system. Therefore, it is the reduction factor for the force determined based upon the linear elastic analysis to estimate the force that would occur when nonlinear behavior is considered. A larger R factor then indicates a more dissipative system. In the case study example discussed in Section 5 of this manuscript, the response modification factor, R was determined as 8 according to ASCE 7 recommendations for the special steel moment frames [1].

Here, we investigate the effect of the selected R factor on the proposed robust design optimization methodology. The analysis of the steel moment resisting frame discussed earlier is performed with varying R values, specifically, $R = 2$, $R = 3$ and $R = 12$. In the genetic algorithm, a population size of 100 is used, the results of which are provided in Fig. 11.

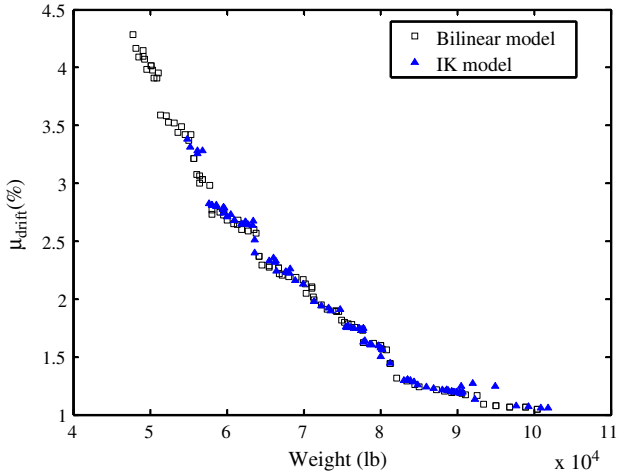

Fig. 9. Pareto front based on bilinear beam model and Pareto front based on IK model.

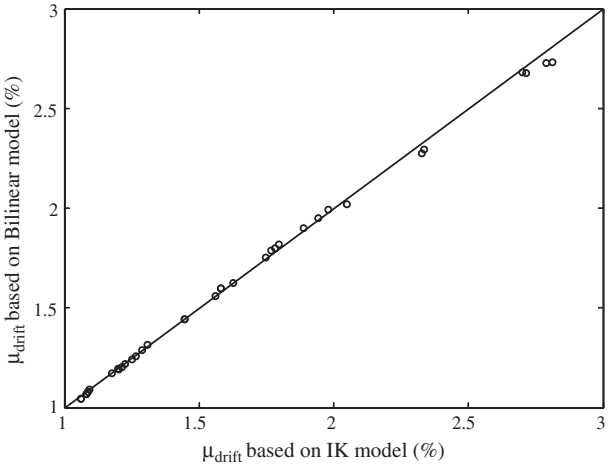

Fig. 10. μ_{drift} calculated based on IK model versus μ_{drift} calculated based on bilinear model for designs in common.

As seen in Fig. 11, a larger R factor introduces a larger reduction in the seismic force, thus posing a less strict requirement on the strength of the system. Hence, the feasible design space for a higher R factor encompasses the feasible design space for a lower R factor. As shown in Fig. 11, the weight and μ_{drift} of Pareto front solutions of $R = 8$ spread within a wider range compared to that of $R = 3$ (Fig. 11(b)), and the weight and μ_{drift} of Pareto front solutions of $R = 12$ spread within a wider range compared to that of $R = 8$ (Fig. 11(c)).

The number of coinciding designs for the Pareto front solutions with $R = 3$ (Fig. 11(b)) and that with $R = 8$ was 52, indicating that those solutions obtained with $R = 8$ can satisfy a much stricter strength requirement ($R = 3$). However, as the R is reduced to 2, the Pareto front solutions that are feasible for $R = 8$ no longer remain so (Fig. 11(a)), clearly indicating that no Pareto front solutions obtained with $R = 2$ coincide with that obtained with $R = 8$. As the feasible solution space for $R = 2$ is contained by that for $R = 8$, the Pareto front solutions for $R = 2$ are dominated by that for $R = 8$, i.e., for identical weight, the μ_{drift} is larger.

7. Conclusions

In this paper, the authors detailed their performance based robust design optimization of steel moment resisting frame, with cost, mean value of seismic demand and standard deviation of seismic demand the three objectives, with the ground motion variability as the noise factor, and with steel section sizes sought to minimize the objectives. A four-story three-bay steel moment resisting frame was used to demonstrate the proposed methodology, and the influence of connection behavior and response modification factors on Pareto front solutions were studied.

The authors determined the use of the methodology in obtaining a set of competing designs that are economical, safe and robust in the form of a Pareto front, with which structural engineers and stakeholders can make decisions informed about the tradeoffs between these three aspects.

The Pareto front designs are found superior to dominated designs in terms of cost, safety and robustness, compared to the traditional trial-and-error method that is likely to yield a dominated (inefficient) design rather than a Pareto front (efficient) design as Pareto optimal designs only occupy a small proportion of the solution space. For identical mean value of seismic demand, variation of seismic demand can be reduced through adjusting design variables and a safer design can be achieved.

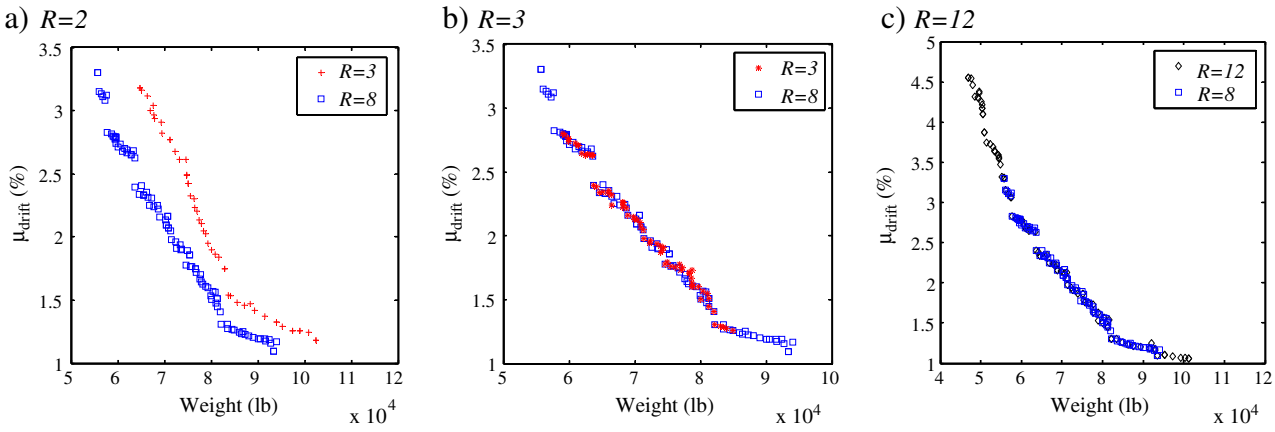

Fig. 11. Pareto front obtained based on several sets of assumed *R* factors.

The uniformity drift ratio was deemed an effective design efficiency indicator in that the efficient designs generally exhibited a smaller uniformity ratio, whereas their inefficient counterparts exhibited a larger uniformity drift ratio. Required uniformity drift ratio for each range of maximum inter-story drift for ensuring efficient designs was suggested. With the suggested requirement enforced, efficient designs can be achieved with the trial and error process without complex optimization.

The Pareto front solution was just marginally influenced by the selected connection model. The Pareto front based on $R = 8$, satisfied the much stricter strength requirement with a smaller *R* factor ($R = 3$). Pareto front solutions with a greater *R* factor were observed to dominate solutions obtained with a lesser *R* factor.

The concepts described in this manuscript can be straightforwardly implemented using many other design codes. Thus, future study is recommended to further develop this approach according to other building codes (e.g. Eurocode). Though ground motion variability is the dominating uncertainty in the seismic design of structures, other uncertainties that not considered here can also cause variations in seismic demand. Therefore, future research should involve an analysis of the connection model uncertainty, and mass and damping ratio uncertainties as concerns our model developed here.

References

[1] American Society of Civil Engineers. ASCE-7 minimum design loads for buildings, Reston, VA; 2010 .
[2] American Institute of Steel Construction. Specification for structural steel buildings, ANSI/AISC 360-10. Chicago: American Institute of Steel Construction; 2010 .
[3] Federal Emergency Management Agency (FEMA). Recommended seismic design criteria for new steel moment-frame buildings: Rep. No. FEMA-350. Washington, D.C.: SAC Joint Venture for FEMA; 2000
[4] Xu L, Grierson DE. Computer-automated design of semirigid steel frameworks. J Struct Eng 1993;119(6):1740–60.
[5] Kameshki ES, Saka MP. Genetic algorithm based optimum design of nonlinear planar steel frames with various semi-rigid connections. J Constr Steel Res 2003;59(1):109–34.
[6] Kargahi M, Anderson JC, Dessouky MM. Structural weight optimization of frames using tabu search. I: optimization procedure. J Struct Eng 2006;132(12):1858–68.
[7] Kaveh A, Farahmand Azar B, Hadidi A, Rezazadeh Sorochi F, Talatahari S. Performance-based seismic design of steel frames using ant colony optimization. J Constr Steel Res 2010;66(4):566–74.
[8] Sarma KC, Adeli H. Life-cycle cost optimization of steel structures. Int J Numer Methods Eng 2002;55(12):1451–62.
[9] Liu M, Burns SA, Wen YK. Optimal seismic design of steel frame buildings based on life cycle cost considerations. Earthq Eng Struct Dyn 2003;32:1313–32.
[10] Liu M, Burns SA, Wen YK. Multiobjective optimization for performance-based seismic design of steel moment frame structures. Earthq Eng Struct Dyn 2005;34(3):289–306.
[11] Fragiadakis M, Lagaros ND, Papadrakakis M. Performance-based multiobjective optimum design of steel structures considering life-cycle cost. Struct Multidiscip Optim 2006;32:1–11.
[12] Rojas HA, Foley C, Pezeshk S. Risk-based seismic design for optimal structural and nonstructural system performance. Earthq Spectra 2011;27(3):857–80.
[13] Taguchi G. Introduction to quality engineering: designing quality into products and processes. Quality resources. NY: White Plains; 1986 .
[14] Phadke MS. Quality engineering using robust design. NJ: Prentice Hall; 1989 .
[15] Park Gyung-Jin, Lee Tae-Hee, Lee Kwon Hee, Hwang K-H. Robust design: an overview. AIAA J 2006;44(1):181–91.
[16] Nair VN, Abraham B, MacKay J, Nelder JA, Box G, Phadke MS, et al. Taguchi's parameter design: a panel discussion. Technometrics 1992;34(2):127–61.
[17] Beyer H, Sendhoff B. Robust optimization — a comprehensive survey. Comput Methods Appl Mech Eng 2007;196:3190–218.
[18] Wen YK, Ellingwood BR, Veneziano D, Bracci J. Uncertainty modeling in earthquake engineering. Urbana, IL: Mid-America Earthquake Engineering Center; 2003 .
[19] Jalayer Fatemeh, Cornell C Allin. A technical framework for probability-based demand and capacity factor design (DCFD) seismic formats. PEER-2003/08, Pacific Earthquake Engineering Research Center. Berkeley: University of California; 2003 .
[20] Shome N, Cornell CA, Bazzurro P, Carballo JE. Earthquakes, records, and nonlinear responses. Earthq Spectra 1998;14(3):469–500.
[21] Ellingwood BR, Kinali K. Quantifying and communicating uncertainty in seismic risk assessment. Struct Saf 2009;31(2):179–87.
[22] Zadeh LA. Optimality and non-scalar-valued performance criteria. IEEE Trans Autom Control 1963;AC-8:59–60.
[23] Charnes A, Cooper WW. Goal programming and multiple objective optimization. Part 1. Eur J Oper Res 1977;1:39–54.
[24] Chen W, Wiecek M, Zhang J. Quality utility: a compromise programming approach to robust design. ASME J Mech Des 1999;121(2):179–87.
[25] Messac A, Puemi-Sukam C, Melachrinoudis E. Mathematical and pragmatic perspectives of physical programming. AIAA J 2001;39:885–93.
[26] Deb K, Pratap A, Agarwal S. A fast and elitist multiobjective genetic algorithm: NSGA-II. IEEE Trans Evol Comput 2002;6(2):182–97.
[27] Marler RT, Arora JS. Survey of multi-objective optimization methods for engineering. Struct Multidiscip Optim 2004;26(6):369–95.
[28] Somerville P, Smith N, Puntamurthula S, Sun J. Development of ground motion time histories for phase 2 of the FEMA/SAC steel project, SAC background document SAC/BD-97/04. Richmond, CA: SAC Joint Venture; 1997 .
[29] American Society of Civil Engineers. Prestandard and commentary on the seismic rehabilitation of buildings. Rep. No. FEMA 356, Washington, D.C.; 2000.
[30] Applied Technology Council (ATC). Seismic evaluation and retrofit of concrete buildings. Rep. No. ATC-40. Redwood City, Calif.: Applied Technology Council; 1996
[31] Kalkan E, Kunnath SK. Assessment of current nonlinear static procedures for seismic evaluation of buildings. Eng Struct 2007;29(3):305–16.
[32] Applied Technology Council (ATC). Improvement of nonlinear static seismic analysis procedures. Rep. No. FEMA-440, Washington, D.C.; 2005.
[33] Chopra AK, Goel RK. A modal pushover analysis procedure for estimating seismic demands for buildings. Earthq Eng Struct Dyn 2002;31(3):561–82.
[34] Chopra AK, Goel RK, Chintanapakdee C. Evaluation of a modified MPA procedure assuming higher modes as elastic to estimate seismic demands. Earthq Spectra 2004;20(3):757–78.
[35] Ibarra LF, Medina RA, Krawinkler H. Hysteretic models that incorporate strength and stiffness deterioration. Earthq Eng Struct Dyn 2005;34(12):1489–511.
[36] Lignos DG, Krawinkler H. Deterioration modeling of steel components in support of collapse prediction of steel moment frames under earthquake loading. J Struct Eng 2011;137(11):1291–302.
[37] Yun S, Hamburger RO, Cornell CA, Foutch DA. Seismic performance evaluation for steel moment frames. J Struct Eng 2002;128(4):534–45.
[38] Lagaros ND, Papadrakakis M. Robust seismic design optimization of steel structures. Struct Multidiscip Optim 2007;33(6):457–69.
[39] Luco Nicolas, Cornell CAllin. Effects of connection fractures on SMRF seismic drift demands. ASCE J Struct Eng 2000;126(1):127–36.
[40] Foutch DA, Shi S. Connection element (type 10) for DRAIN-2DX. Dept. of Civ. Engr., University of Illinois at Urbana-Champaign, Ill; 1996 .
[41] Sakurai S, Ellingwood BR, Kushiyama S. Probabilistic study of the behavior of steel frames with partially restrained connections. Eng Struct 2001;23:1410.
[42] Kishi N, Chen WF. Moment–rotation relations of semi rigid connections with angles. J Struct Eng ASCE 1990;116(7):1813–33.